INSTITUTE OF PHYSICS PUBLISHING JOURNAL OF PHYSICS: CONDENSED MATTER

J. Phys.: Condens. Matter **18** (2006) 459–478 doi:10.1088/0953-8984/18/2/009

Magnetic anisotropy in the cubic Laves $REFe_2$ intermetallic compounds

K N Martin[1], P A J de Groot[1], B D Rainford[1], K Wang[1], G J Bowden[1,3], J P Zimmermann[2] and H Fangohr[2]

[1] School of Physics and Astronomy, University of Southampton, SO17 1BJ, UK
[2] Computational Engineering and Design Group, School of Engineering Sciences, University of Southampton, SO17 1BJ, UK

E-mail: gjb@phys.soton.ac.uk

Received 14 July 2005, in final form 19 October 2005
Published 14 December 2005
Online at stacks.iop.org/JPhysCM/18/459

Abstract

In the past, the Callen–Callen (1965 *Phys. Rev.* **139** A455–71; 1966 *J. Phys. Chem. Solids* **27** 1271–85) model has been highly successful in explaining the origin and temperature dependence of the magneto-crystalline anisotropy in many magnetic compounds. Yet, despite their high ordering temperatures of ∼650 K, the Callen–Callen model has proved insufficient for the $REFe_2$ compounds. In this paper, we show that it is possible to replicate the values of the phenomenological parameters K_1, K_2, and K_3 given by Atzmony and Dariel (1976 *Phys. Rev.* B **13** 4006–14), by extending the Callen–Callen model to second order in $\mathcal{H}_{\mathrm{CF}}$. In particular, explanations are provided for (i) the unexpected changes in sign of K_1 and K_2 in $HoFe_2$ and $DyFe_2$, respectively, and (ii) the origin and behaviour of the K_3 term. In addition, it is demonstrated that higher order terms are required, and that K_4 exceeds K_3 at low temperatures. Revised estimates of K_1, K_2, K_3, K_4, and K_5 are given. Finally, an alternative 'multipolar' approach to the problem of magnetic anisotropy is also provided. It is shown that the latter confers significant advantages over the older phenomenological method. In particular, all the multipolar coefficients ($\tilde{K}_N$, $N = 4, 6, 8, 10, 12$) decrease monotonically with increasing temperature, with $\tilde{K}_N$ decreasing faster than $\tilde{K}_{N-2}$ etc. These observations are in accord with expectations based on the original Callen–Callen model.

(Some figures in this article are in colour only in the electronic version)

1. Introduction

Recent research into the properties of thin magnetic films grown by molecular beam epitaxy (MBE), has led to a resurgence of interest in the cubic Laves rare-earth intermetallic compounds

[3] Author to whom any correspondence should be addressed.

($REFe_2$). In particular, it has been shown that $REFe_2/YFe_2$ multilayer films can be fabricated which exhibit magnetic exchange springs (Dumesnil *et al* 2000, Sawicki *et al* 2000), negative coercivity (Gordeev *et al* 2001), and giant magneto-resistance (Gordeev *et al* 2001). In general, crystalline MBE grown multilayer films can be used to study a wide variety of problems including exchange-bias phenomena, magnetization reversal, etc (Dumesnil *et al* 2005). The study of such films is important in that they promise applications in the fields of permanent magnets (Coey and Skomski 1993), magnetostrictive devices (Clark 1979), and magnetic field sensors (Gordeev *et al* 2001).

Concomitant with the experimental work, effort has been put into the magnetic modelling of the $REFe_2$ multilayer and other films, to provide an explanation of the sometimes exotic M-Bapp loops (Fullerton *et al* 1999, Amato *et al* 2000, Bowden *et al* 2000, 2003). This in turn has led to a need for accurate magnetic anisotropy parameters K_1 etc for the bulk $REFe_2$ compounds. But, in fact, very few magnetic measurements have been performed on $REFe_2$ single crystals. Instead, values of K_1 etc have been determined indirectly, primarily from experiments on polycrystalline samples. For example, during the mid-1970s, exhaustive ^{57}Fe Mössbauer studies were used to determine the directions of easy magnetization in mixed RE intermetallic compounds of the form $RE(a)_{1-x}RE(b)_xFe_2$ (Atzmony *et al* 1973, 1976, hereafter referred to as A&D). In particular, spin-orientation diagrams (SODs) were prepared, and used to determine values of the crystal field parameters B_4 and B_6, for the differing RE ions. Subsequently, extensive calculations of the free energy F were performed, for 30 directions of magnetization, to obtain F as a function of (θ, ϕ) and of temperature: a *tour de force*. Given these data, values of K_1 etc for the RE ions Tb, Dy, Ho, and Er were extracted using a least squares procedure. It is these values which are currently being used by magnetic modellers working on MBE $REFe_2$ thin films (see table 2 of Mougin *et al* 2000 for selected values of K_1 and K_2).

However, in the work of A&D some distinct surprises were found. In particular, certain alloys were found to possess *non-major* cubic symmetry axes of easy magnetization $[uuv]$ *or* $[uv0]$. This led A&D to propose and justify the existence of an additional K_3 anisotropy term:

$$E_A = K_1[\alpha_x^2\alpha_y^2 + \alpha_x^2\alpha_z^2 + \alpha_y^2\alpha_z^2] + K_2[\alpha_x^2\alpha_y^2\alpha_z^2] + K_3[\alpha_x^4\alpha_y^4 + \alpha_x^4\alpha_z^4 + \alpha_y^4\alpha_z^4] \tag{1}$$

where the α_x etc are the direction cosines. Given just K_1 and K_2 it is easily shown that only the *major* cubic axes [001], [101], and [111] are allowed directions of easy magnetization. For *non-major*$[uuv]$ or $[uv0]$ directions a K_3 term is required. Such a term had been seen earlier in very careful measurements on a single crystal of nickel (Aubert 1968). However, in the $REFe_2$ compounds this term is much larger and cannot be ignored. To quote A&D,

Several points of interest should be noted. (i) K_3 is found to be positive for all the investigated RE ions. (ii) K_3 is of the same order of magnitude as K_1 and K_2 at low temperatures. (iii) K_1 in $HoFe_2$ *and K_2 in* ($DyFe_2$) *change sign as the temperature is increased*.

While A&D offer no comment concerning the last point, it is surprising. For many years the Callen–Callen (C&C) model of magnetic anisotropy has been highly successful in the interpretation of many RE compounds (C&C 1966). This model predicts that the anisotropy parameters decrease monotonically with increasing temperature. But in the case of $HoFe_2$($DyFe_2$), respectively, the calculations of A&D show that K_1 (K_2) changes sign very rapidly over a very narrow temperature range $\sim$20 K.

In this paper, we show that even in the $REFe_2$ compounds, which possess very high Néel temperatures of 650 K, the C&C model is not sufficient. In practice, it is necessary to go beyond 'first order perturbation theory' to understand the magnetic anisotropy of these compounds.

The improved theory provides a clear explanation of all the points raised by A&D, especially the unexpected changes in sign of K_1 in $HoFe_2$ and K_2 in $DyFe_2$. The origin and behaviour of the K_3 term is also clearly identified. However, it is also shown that higher order terms K_4 and K_5 terms are present and cannot be ignored. Revised values of K_1, K_2, K_3, K_4, and K_5 are presented and discussed.

Finally, it is argued that the alternative multipolar approach to magnetic anisotropy confers significant advantages over the phenomenological method. For example, all the multipolar coefficients $\tilde{K}_N$ ($N = 4, 6, 8, 10, 12$) decrease monotonically with increasing temperature, in accord with expectations based on the original C&C model.

2. The Hamiltonian for the RE ion in the $REFe_2$ compounds

In common with previous authors we shall assume that the dominant anisotropy in the $REFe_2$ compounds derives from the crystal field interaction at the RE ions, with the exceptions of Gd and Y.

Following Cohen (1964), Bowden *et al* (1968), Atzmony *et al* (1973), and Atzmony and Dariel (1976), the Hamiltonian at the RE ion can be written

$$\mathcal{H} = \mathcal{H}_{\mathrm{Ex}} + \mathcal{H}_{\mathrm{CF}} \tag{2}$$

where (i)

$$\mathcal{H}_{\mathrm{Ex}} = 2(g_j - 1)\mu_{\mathrm{B}} H_{\mathrm{EX}}^{\mathrm{Fe}} J_Z = X J_Z \tag{3}$$

and (ii)

$$\mathcal{H}_{\mathrm{CF}} = B_4[O_{40} + 5O_{44}^C] + B_6[O_{60} - 21 O_{64}^C]. \tag{4}$$

Here (i) the exchange field $H_{\mathrm{EX}}^{\mathrm{Fe}}$ at the RE site is assumed to follow the temperature dependence of the Fe sub-lattice, as determined by the ^{57}Fe Mössbauer effect, and (ii) B_4 and B_6 are the crystal field coefficients at the RE site (see for example Abragam and Bleaney 1970, Hutchings 1964). In passing, we note that we have chosen X to symbolize the close connection with the C&C model, as applied say to the RE metals. In the latter, the temperature dependent effective field X is determined from the measured magnetization curve $M(T)$, via an inverse Langevin function. However, in the case of the $REFe_2$ compounds, the magnetic exchange field at the RE site is generated primarily by the transition metal sub-lattice. In this case, therefore, there is no need to measure M(RE) and invoke the inverse Langevin function. However, in other Laves phase compounds, such as the $REAl_2$ compounds, it will be necessary to determine X from magnetization measurements, in the usual way. With this proviso therefore, the theory presented below could be applied to such compounds.

In their paper, A&D set $\mu_{\mathrm{B}} H_{\mathrm{EX}}^{\mathrm{Fe}}(T = 0\ \mathrm{K}) = 150$ K and constant up to 300 K. In this work however, we allow $H_{\mathrm{EX}}^{\mathrm{Fe}}$ to follow the temperature dependence of the Fe sub-lattice, as determined by the ^{57}Fe Mössbauer effect. But it should be noted that A&D remark that their SOD curves are not greatly affected by an increase of $\mu_{\mathrm{B}} H_{\mathrm{EX}}^{\mathrm{Fe}}$ by some 50%. From measurements on the ^{161}Dy magnetic and quadrupole fields, Bowden *et al* (1968) find $\mu_{\mathrm{B}} H_{\mathrm{EX}}^{\mathrm{Fe}}(T = 0\ \mathrm{K}) = 202(7)$ K, some 35% higher than the estimate given by A&D. This figure has recently been confirmed, from magnetostriction studies on $DyFe_2$ (Bowden *et al* 2004). On the other hand, using the Mössbauer effect in ^{169}Tm, Bleaney *et al* (1981) find $\mu_{\mathrm{B}} H_{\mathrm{EX}}^{\mathrm{Fe}}(T = 0\ \mathrm{K}) = 153(3)$ K, in good accord with the A&D estimate. In this paper, we set $\mu_{\mathrm{B}} H_{\mathrm{EX}}^{\mathrm{Fe}}(T = 0\ \mathrm{K}) = 150$ K, for all the REs, primarily for comparative purposes. We turn now to a discussion of the crystal field Hamiltonian.

For historical reasons, the crystal field Hamiltonian for an RE ion in the $REFe_2$ compounds is often written in the form of equation (4). However, even in the early days an alternative

Table 1. The RE ion parameters derived from A&D and references contained therein. The units are K/ion.

RE	B_4	B_6	X
Tb	$+6.45 \times 10^{-3}$	$+8.73 \times 10^{-6}$	150
Dy	-3.02×10^{-3}	-7.22×10^{-6}	100
Ho	-1.15×10^{-3}	$+8.03 \times 10^{-6}$	75
Er	$+1.86 \times 10^{-3}$	-1.13×10^{-6}	60
Tm	$+6.33 \times 10^{-3}$	$+2.72 \times 10^{-6}$	50

set of operators $\tilde{\mathbf{O}}_q^n$ was proposed by Smith and Thornley (1966), which is more useful when rotations of the co-ordinate system are required. This comment also applies to the set of tensor operators $\mathbf{T}_q^n$ given by Buckmaster *et al* (1972). The latter differ from those of Smith and Thornley in the definition of the reduced matrix element, but the formulation of Buckmaster *et al* carries additional advantages. Firstly, it is possible to construct the entire tensor set starting from the basic building blocks $\mathbf{T}_0^1$, $\mathbf{T}_{-1}^1$, $\mathbf{T}_{+1}^1$. Secondly, the operators can be recast in terms of unit irreducible tensor operators $\hat{\mathbf{T}}_q^n$, where $\mathrm{Tr}[\hat{\mathbf{T}}_q^n(\hat{\mathbf{T}}_{q'}^{n'})^*] = \delta_{nn'}\delta_{qq'}$. Such products arise in second order perturbation theory (see equations (13) and (14) below and appendix A). Finally, formulae exist for recasting products of tensor operators $\hat{\mathbf{T}}_q^n\hat{\mathbf{T}}_{q'}^{n'}$ into single tensors $\hat{\mathbf{T}}_Q^N$, where $\mathbf{N} \leqslant \mathbf{n} + \mathbf{n}'$ (Bowden and Hutchison 1986).

Within the Buckmaster formulation therefore the crystal field takes the form

$$\mathcal{H}_{\mathrm{CF}} = \tilde{B}_4\left[\mathbf{T}_0^4 + \sqrt{\tfrac{5}{14}}(\mathbf{T}_4^4 + \mathbf{T}_{-4}^4)\right] + \tilde{B}_6\left[\mathbf{T}_0^6 - \sqrt{\tfrac{7}{2}}(\mathbf{T}_4^6 + \mathbf{T}_{-4}^6)\right] \tag{5}$$

where

$$\tilde{B}_4 = 2\sqrt{70}B_4 \qquad \text{and} \qquad \tilde{B}_6 = 4\sqrt{231}B_6. \tag{6}$$

In passing we note the spin operators $\mathbf{T}_m^n$ are closely related to the Racah operators:

$$\tilde{\mathbf{U}}_m^n = \sqrt{\frac{4\pi}{2n+1}}Y_n^m(\theta, \phi) \tag{7}$$

with well known rotational properties (e.g. Edmonds 1957).

The set of parameters used in this work is set out in table 1. We are now in a position to develop the theory of magnetic anisotropy as presented by Callen and Callen (1965, 1966) and Callen and Shtrikman (1965).

3. The Callen–Callen model: first order perturbation theory

In the next two sections, we follow the first and second order perturbation theory as given by Bowden (1977) for the heavy RE metals, but this time applied to the cubic Laves $REFe_2$ compounds. Readers who are not interested in the details should skip to the final result embodied in equation (19).

Provided the crystal field Hamiltonian is small compared to the magnetic exchange, the free energy of the RE ion can be expanded in the form

$$F = F_0 + F' + F'' + \cdots \tag{8}$$

where $F_0 = F_{\mathrm{EX}}$ is the free energy associated with the 'dominant' magnetic exchange term, and $F' = \langle\mathcal{H}_{\mathrm{CF}}\rangle_{\mathrm{EX}}$ etc. In this paper the use of a single (double) prime on any symbol refers to its origin as being derived from first (second) order perturbation theory, respectively.

For an arbitrary direction of magnetization, we find from equation (28) of Bowden (1977)

$$F' = \langle H_{CF}\rangle_{EX} = \sum_{n,m} \tilde{B}^n_m \mathcal{D}^n_{0m}(\omega)\langle \mathbf{T}^n_0\rangle_{EX} \tag{9}$$

where (i) the $\mathcal{D}^n_{0m}(\omega)$ are the well known rotation operators (Edmonds 1957), (ii) ω is a shorthand notation for the Euler angles (α, β, γ), and (iii) the expectation values are calculated using the eigenvalues and Zeeman functions of the magnetic exchange. Explicitly,

$$\langle T^n_0\rangle = \mathrm{Tr}[T^n_0\rho] = \sum_m \langle m|\mathbf{T}^n_0|m\rangle \exp[-\beta X m] \Big/ \sum_m \exp[-\beta X m]. \tag{10}$$

From here on in, we shall drop the exchange suffix on all expectation values.

On specializing to the $REFe_2$ compounds therefore we find

$$\begin{aligned} F' = {} & \tilde{K}'_4(T)\Big[Y^0_4(\theta,\phi) + \sqrt{\tfrac{5}{14}}\big(Y^4_4(\theta,\phi) + Y^{-4}_4(\theta,\phi)\big)\Big] \\ & + \tilde{K}'_6(T)\Big[Y^0_6(\theta,\phi) - \sqrt{\tfrac{7}{2}}\big(Y^4_6(\theta,\phi) + Y^{-4}_6(\theta,\phi)\big)\Big] \end{aligned} \tag{11}$$

where we have noted that (i) $\mathcal{D}^n_{0n}(\omega)$ is independent of α, (ii) we have set (β, γ) equal to (θ, ϕ), respectively, and (iii) there is a simple relationship between the $\mathcal{D}^n_{0m}(\theta, \phi)$ and the spherical harmonics $Y^m_n(\theta, \phi)$ (Edmonds 1957). Finally, the temperature anisotropy constants appearing in equation (11) are given by

$$\begin{aligned} \tilde{K}'_4(T) &= \sqrt{\frac{4\pi}{9}}\,\tilde{B}^4_0\langle \mathbf{T}^4_0\rangle \\ \tilde{K}'_6(T) &= \sqrt{\frac{4\pi}{13}}\,\tilde{B}^6_0\langle \mathbf{T}^6_0\rangle. \end{aligned} \tag{12}$$

This is the principal result of the Callen and Callen (1966) model of anisotropy. The expectation values $\langle \mathbf{T}^4_0\rangle$ and $\langle \mathbf{T}^6_0\rangle$ decrease monotonically with increasing temperature and do not change sign. Moreover, at low temperatures $\langle \mathbf{T}^6_0\rangle$ falls off more rapidly than $\langle \mathbf{T}^4_0\rangle$, in accord with the $\sigma(T)^{n(n+1)/2}$ law (Akulov 1936), where $\sigma(T)$ is the reduced magnetization. Most authors have stopped here.

4. The extended Callen–Callen model: second order perturbation theory

From equation (47) of Bowden (1977), but using Buckmaster's tensor operators, we find

$$\begin{aligned} F'' = {} & -\tfrac{1}{2}\beta\Bigg\{\sum_{n,m}\sum_{n',m'} \tilde{B}^n_m \tilde{B}^{n'}_m \sum_{N,M}(2N+1)\begin{pmatrix} n & n' & N \\ m & m' & M\end{pmatrix}\mathcal{D}^N_{0M}(\omega)^* \\ & \times \sum_q \begin{pmatrix} n & n' & N \\ q & -q & 0\end{pmatrix}\langle \mathbf{T}^n_q \vdots \mathbf{T}^{n'}_{-q}\rangle\Bigg\} \end{aligned} \tag{13}$$

where $\langle \mathbf{T}^n_q \vdots \mathbf{T}^{n'}_{q'}\rangle$ is a shorthand notation for

$$\begin{aligned} \langle \mathbf{T}^n_q \vdots \mathbf{T}^{n'}_{q'}\rangle &= \left\langle \mathbf{T}^n_q \int \mathbf{T}^{n'}_{q'}\right\rangle - \langle \mathbf{T}^n_q\rangle\langle \mathbf{T}^{n'}_{q'}\rangle \\ &= \mathrm{Tr}\left[\mathbf{T}^n_q \int_0^1 \mathrm{d}s\, \rho^{1-s}\mathbf{T}^{n'}_{q'}\rho^s\right] - \langle \mathbf{T}^n_q\rangle\langle \mathbf{T}^{n'}_{q'}\rangle \end{aligned} \tag{14}$$

and $\beta = 1/kT$. In practice, it is advantageous to recast equation (13) in the form

$$F'' = -\tfrac{1}{2}\beta\Bigg\{\sum_{n,m}\sum_{n',m'} \tilde{B}^n_m \tilde{B}^{n'}_m \sum_{N,M}(2N+1)\begin{pmatrix} n & n' & N \\ m & m' & M\end{pmatrix}\mathcal{D}^N_{0M}(\omega)^*\alpha_{n,n',N}(T)\Bigg\} \tag{15}$$

where the $\alpha_{n,n',N}(T)$ coefficients are given by

$$\alpha_{n,n',N}(T) = \sum_q \begin{pmatrix} n & n' & N \\ q & -q & 0 \end{pmatrix} \langle \mathbf{T}^n_q \vdots \mathbf{T}^{n'}_{-q} \rangle. \tag{16}$$

Note that the temperature dependence of the second order terms is governed by that of the $\alpha_{n,n',N}(T)$ coefficients, via the $\langle \mathbf{T}^n_q \vdots \mathbf{T}^{n'}_{-q} \rangle$ ensemble averages, together with the global $\beta = 1/kT$ term appearing outside all of the terms in equation (15). In practice, all the $\beta\alpha_{n,n',N}(T)$ coefficients converge uniformly to zero as the temperature is increased. Details concerning the properties of the $\alpha_{n,n',N}(T)$ can be found in appendix A.

In all there are 44 terms to consider, but only 14 are non-zero. It is also advantageous to gather those terms with the same rank N (=0, 4, 6, 8, 10, and 12), since this allows clear identification of the multipolar nature of the cubic combinations of spherical harmonics.

5. Results for the $REFe_2$ compounds

From equation (13) it is clear that second order perturbation theory will lead to terms which are proportional to $(\tilde{B}_4)^2$, $(\tilde{B}_6)^2$ and the cross terms $(\tilde{B}_4)(\tilde{B}_6)$. These give rise to a rich spectrum of terms. In particular, $(\tilde{B}_4)^2$ give rise to spherical harmonics with rank $\leqslant 8$, $(\tilde{B}_4)(\tilde{B}_6)$ to spherical harmonics with rank $\leqslant 10$, and $(\tilde{B}_6)^2$ to spherical harmonics with rank $\leqslant 12$, respectively.

As an example, consider the second order term involving $(\tilde{B}_4)^2$. We find

$$\begin{aligned} F''(4,4) = {} & \tilde{K}''_{440}(T) Y^0_0(\theta,\phi) \\ & + \tilde{K}''_{444}(T)\left[Y^0_4(\theta,\phi) + \sqrt{\tfrac{5}{14}}(Y^4_4(\theta,\phi) + Y^{-4}_4(\theta,\phi)) \right] \\ & + \tilde{K}''_{446}(T)\left[Y^0_6(\theta,\phi) - \sqrt{\tfrac{7}{2}}(Y^4_6(\theta,\phi) + Y^{-4}_6(\theta,\phi)) \right] \\ & + \tilde{K}''_{448}(T)\left[Y^0_8(\theta,\phi) + \tfrac{1}{3}\sqrt{\tfrac{14}{11}}(Y^4_8(\theta,\phi) + Y^{-4}_8(\theta,\phi)) \right. \\ & \left. + \tfrac{1}{3}\sqrt{\tfrac{65}{22}}(Y^8_8(\theta,\phi) + Y^{-8}_8(\theta,\phi)) \right] \end{aligned} \tag{17}$$

where the $\tilde{K}''_{nn'N}(T)$ coefficients are given by the first four rows of table 2.

The first term (N = rank zero) is a constant and need not concern us. The next two terms are the usual rank four and six cubic harmonics, but this time appearing in second order perturbation theory. The fourth term is new. It is of rank eight but with cubic symmetry. As we shall see below, it is the principal contributor to the phenomenological K_3 term, required by A&D. Note that the series terminates at $N = 8$, by virtue of the $3j$-coefficients appearing in equation (13). Finally, for brevity, we rewrite equation (17) in the more compact form:

$$F''(4,4) = \tilde{K}''_{440}(T) Y^0_0(\theta,\phi) + \tilde{K}''_{444}(T)\mathbf{Y}^C_4(\theta,\phi) + \tilde{K}''_{446}(T)\mathbf{Y}^C_6(\theta,\phi) + \tilde{K}''_{448}(T)\mathbf{Y}^C_8(\theta,\phi) \tag{18}$$

where the cubic combinations of spherical harmonics are listed in table 3.

Finally, on gathering both the first and second order terms, the anisotropy energy can be written in the concise form

$$\begin{aligned} E_A = F' + F'' = {} & \tilde{K}_0(T)\left[Y^0_0(\theta,\phi) \right] \\ & + \tilde{K}_4(T)\mathbf{Y}^C_4 + \tilde{K}_6(T)\mathbf{Y}^C_6 + \tilde{K}_8(T)\mathbf{Y}^C_8 + \tilde{K}_{10}(T)\mathbf{Y}^C_{10} + \tilde{K}_{12}(T)\mathbf{Y}^C_{12} \end{aligned} \tag{19}$$

Table 2. The second order anisotropy coefficients. Both the cross terms $\tilde{B}_4\tilde{B}_6$ and $\tilde{B}_6\tilde{B}_4$ have been included, in the definition of the $K''_{46N}(T)$ coefficients.

$$\tilde{K}''_{440}(T) = -\tfrac{1}{2}\beta\left[+\tfrac{4\sqrt{4\pi}}{7}(\tilde{B}_4)^2\alpha_{440}(T)\right]$$
$$\tilde{K}''_{444}(T) = -\tfrac{1}{2}\beta\left[+\sqrt{\tfrac{4\pi}{9}}\,\tfrac{6\sqrt{14}}{\sqrt{11\cdot13}}(\tilde{B}_4)^2\alpha_{444}(T)\right]$$
$$\tilde{K}''_{446}(T) = -\tfrac{1}{2}\beta\left[-\sqrt{\tfrac{4\pi}{13}}\,\tfrac{4}{7}\sqrt{\tfrac{65}{11}}(\tilde{B}_4)^2\alpha_{446}(T)\right]$$
$$\tilde{K}''_{448}(T) = -\tfrac{1}{2}\beta\left[+\sqrt{\tfrac{4\pi}{17}}\,\tfrac{3}{7}\sqrt{\tfrac{5\cdot11\cdot17}{26}}(\tilde{B}_4)^2\alpha_{448}(T)\right]$$
$$\tilde{K}''_{464}(T) = -\tfrac{1}{2}\beta\left[-\sqrt{\tfrac{4\pi}{9}}\,\tfrac{48\sqrt{5}}{\sqrt{11\cdot13}}\tilde{B}_4\tilde{B}_6\alpha_{464}(T)\right]$$
$$\tilde{K}''_{466}(T) = -\tfrac{1}{2}\beta\left[-\sqrt{\tfrac{4\pi}{13}}\,\tfrac{6\sqrt{7\cdot13}}{\sqrt{11\cdot17}}\tilde{B}_4\tilde{B}_6\alpha_{466}(T)\right]$$
$$\tilde{K}''_{468}(T) = -\tfrac{1}{2}\beta\left[-\sqrt{\tfrac{4\pi}{17}}\,\tfrac{2\sqrt{11\cdot14\cdot17}}{\sqrt{13\cdot19}}\tilde{B}_4\tilde{B}_6\alpha_{468}(T)\right]$$
$$\tilde{K}''_{4610}(T) = -\tfrac{1}{2}\beta\left[+\sqrt{\tfrac{4\pi}{21}}\,\tfrac{3\sqrt{7\cdot10\cdot13}}{\sqrt{17\cdot19}}\tilde{B}_4\tilde{B}_6\alpha_{4610}(T)\right]$$
$$\tilde{K}''_{660}(T) = -\tfrac{1}{2}\beta\left[+\tfrac{8\sqrt{4\pi}}{\sqrt{13}}(\tilde{B}_6)^2\alpha_{660}(T)\right]$$
$$\tilde{K}''_{664}(T) = -\tfrac{1}{2}\beta\left[-\sqrt{\tfrac{4\pi}{9}}\,\tfrac{9\cdot14\sqrt{7}}{\sqrt{11\cdot13\cdot17}}(\tilde{B}_6)^2\alpha_{664}(T)\right]$$
$$\tilde{K}''_{666}(T) = -\tfrac{1}{2}\beta\left[+\sqrt{\tfrac{4\pi}{13}}\,\tfrac{8\sqrt{13}}{\sqrt{11\cdot17\cdot19}}(\tilde{B}_6)^2\alpha_{666}(T)\right]$$
$$\tilde{K}''_{668}(T) = -\tfrac{1}{2}\beta\left[+\sqrt{\tfrac{4\pi}{17}}\,\tfrac{9\sqrt{7\cdot11\cdot17}}{\sqrt{2\cdot13\cdot19}}(\tilde{B}_6)^2\alpha_{668}(T)\right]$$
$$\tilde{K}''_{6610}(T) = -\tfrac{1}{2}\beta\left[+\sqrt{\tfrac{4\pi}{21}}\,\tfrac{35\sqrt{3\cdot7\cdot13}}{\sqrt{17\cdot19\cdot23}}(\tilde{B}_6)^2\alpha_{6610}(T)\right]$$
$$\tilde{K}''_{6612}(T) = -\tfrac{1}{2}\beta\left[+\sqrt{\tfrac{4\pi}{25}}\,\tfrac{5\cdot9\cdot11\sqrt{7}}{\sqrt{13\cdot17\cdot19\cdot23}}(\tilde{B}_6)^2\alpha_{6612}(T)\right]$$

Table 3. Combinations of spherical harmonics with cubic symmetry.

$$\mathbf{Y}^C_4(\theta,\phi) = \left[Y^0_4(\theta,\phi) + \sqrt{\tfrac{5}{14}}(Y^4_4(\theta,\phi) + Y^{-4}_4(\theta,\phi))\right]$$
$$\mathbf{Y}^C_6(\theta,\phi) = \left[Y^0_6(\theta,\phi) - \sqrt{\tfrac{7}{2}}(Y^4_6(\theta,\phi) + Y^{-4}_6(\theta,\phi))\right]$$
$$\mathbf{Y}^C_8(\theta,\phi) = \left[Y^0_8(\theta,\phi) + \tfrac{1}{3}\sqrt{\tfrac{14}{11}}(Y^4_8(\theta,\phi) + Y^{-4}_8(\theta,\phi)) + \tfrac{1}{3}\sqrt{\tfrac{65}{22}}(Y^8_8(\theta,\phi) + Y^{-8}_8(\theta,\phi))\right]$$
$$\mathbf{Y}^C_{10}(\theta,\phi) = \left[Y^0_{10}(\theta,\phi) - \sqrt{\tfrac{66}{65}}(Y^4_{10}(\theta,\phi) + Y^{-4}_{10}(\theta,\phi)) - \sqrt{\tfrac{11\cdot17}{10\cdot13}}(Y^8_{10}(\theta,\phi) + Y^{-8}_{10}(\theta,\phi))\right]$$
$$\mathbf{Y}^C_{12}(\theta,\phi) = \left[Y^0_{12}(\theta,\phi) - \tfrac{4}{9}\sqrt{\tfrac{99}{11}}(Y^4_{12}(\theta,\phi) + Y^{-4}_{12}(\theta,\phi)) + \tfrac{1}{3}\sqrt{\tfrac{13\cdot17\cdot19}{66}}(Y^8_{12}(\theta,\phi) + Y^{-8}_{12}(\theta,\phi))\right]$$

where

$$\begin{aligned}
\tilde{K}_0(T) &= \tilde{K}''_{440}(T) + \tilde{K}''_{660}(T)\\
\tilde{K}_4(T) &= \tilde{K}'_4(T) + \tilde{K}''_{444}(T) + \tilde{K}''_{464}(T) + \tilde{K}''_{664}(T)\\
\tilde{K}_6(T) &= \tilde{K}'_6(T) + \tilde{K}''_{446}(T) + \tilde{K}''_{466}(T) + \tilde{K}''_{666}(T)\\
\tilde{K}_8(T) &= \tilde{K}''_{448}(T) + \tilde{K}''_{468}(T) + \tilde{K}''_{668}(T)\\
\tilde{K}_{10}(T) &= \tilde{K}''_{4610}(T) + \tilde{K}''_{6610}(T)\\
\tilde{K}_{12}(T) &= \tilde{K}''_{6612}(T).
\end{aligned} \tag{20}$$

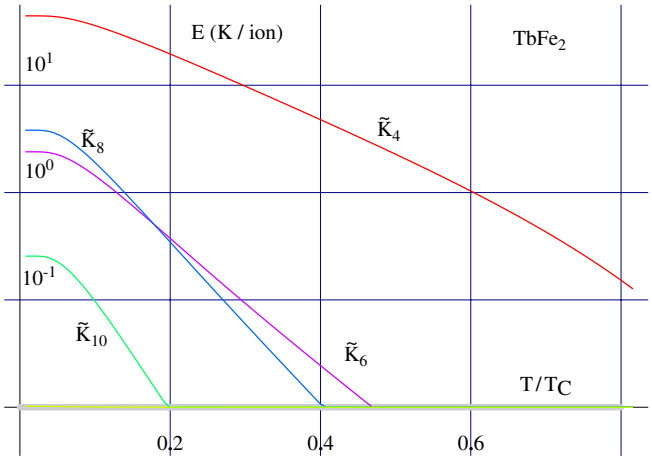

Figure 1. The calculated bulk multipolar magnetic anisotropy constants $\tilde{K}_4$ to $\tilde{K}_{12}$ for $TbFe_2$, plotted logarithmically, as a function of reduced temperature T/T_C. The thick line corresponds to the region $-10^{-2} \leqslant |\tilde{K}_i| \leqslant +10^{-2}$.

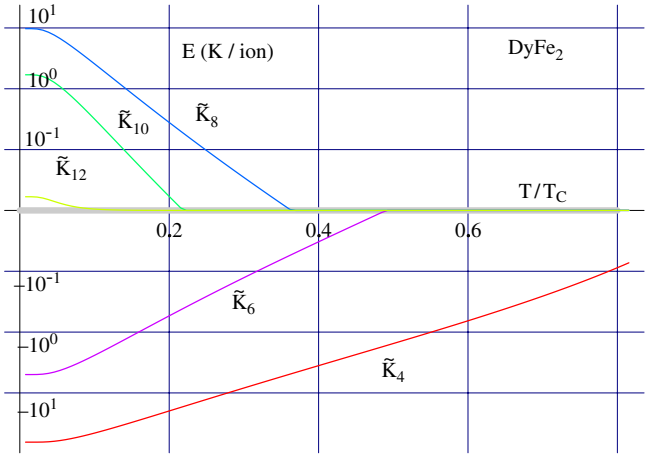

Figure 2. The calculated bulk multipolar magnetic anisotropy constants $\tilde{K}_4$ to $\tilde{K}_{12}$ for $DyFe_2$, plotted logarithmically, as a function of reduced temperature T/T_C. The thick line corresponds to the region $-10^{-2} \leqslant |\tilde{K}_i| \leqslant +10^{-2}$.

Equation (19) represents the extended theory of the Callen–Callen model, in multipolar form. Note that only the fourth and sixth rank $\tilde{K}_4(T)$ and $\tilde{K}_6(T)$ terms have contributions from both first and second order perturbation theory. The first order terms are given by equation (12), while the second order terms $\tilde{K}''_{nn'N}(T)$ are summarized in table 1.

6. Multipolar anisotropy coefficients: calculations

Logarithmic plots of the multipolar coefficients $\tilde{K}_4$–$\tilde{K}_{12}$ can be seen in figures 1–5, as a function of the reduced temperature T/T_C. It will be observed that (i) all the multipolar coefficients decrease monotonically with increasing temperature, (ii) in every case $\tilde{K}_N$ reaches 'zero' ($|\tilde{K}_N| \leqslant 10^{-2}$) faster than $\tilde{K}_{N-2}$, in accord with expectations based on the original C&C

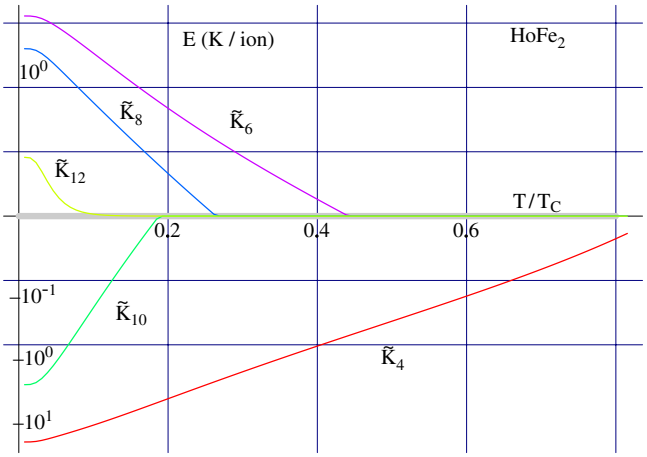

Figure 3. The calculated bulk multipolar magnetic anisotropy constants $\tilde{K}_4$ to $\tilde{K}_{12}$ for $HoFe_2$, plotted logarithmically, as a function of reduced temperature T/T_C. The thick line corresponds to the region $-10^{-2} \leqslant |\tilde{K}_i| \leqslant +10^{-2}$.

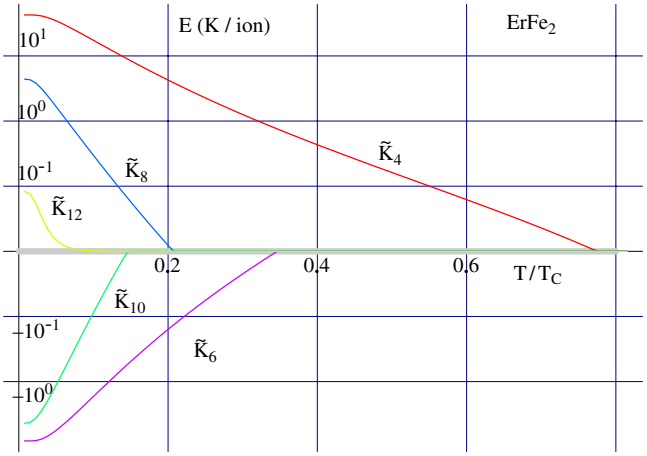

Figure 4. The calculated bulk multipolar magnetic anisotropy constants $\tilde{K}_4$ to $\tilde{K}_{12}$ for $ErFe_2$, plotted logarithmically, as a function of reduced temperature T/T_C. The thick line corresponds to the region $-10^{-2} \leqslant |\tilde{K}_i| \leqslant +10^{-2}$.

model. These calculations are more complete than those of A&D in that they include the higher order terms $\tilde{K}_{10}$ and $\tilde{K}_{12}$. In their paper, A&D warn that the inclusion of still higher order terms may be important. This comment finds a natural resonance in this work. For example, at low temperatures in both $HoFe_2$ and $ErFe_2$, $\tilde{K}_{10} \sim \tilde{K}_8$. Clearly, higher order terms are important. Finally, we note that it is possible to obtain analytic results for the intercepts of $\tilde{K}_N$ at $T = 0$ K. Some expressions for $DyFe_2$ are given in appendix A.

In the next section we forge the link between the multi-polar approach of equations (19) and the phenomenological method embodied in equation (1).

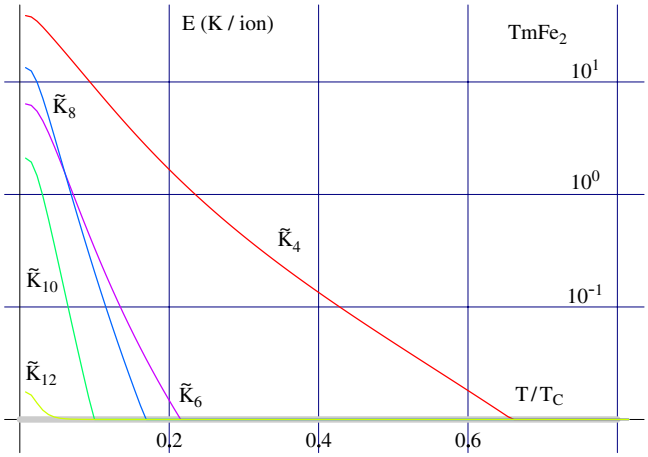

Figure 5. The calculated bulk multipolar magnetic anisotropy constants $\tilde{K}_4$ to $\tilde{K}_{12}$ for $TmFe_2$, plotted logarithmically, as a function of reduced temperature T/T_C. The thick line corresponds to the region $-10^{-2} \leqslant |\tilde{K}_i| \leqslant +10^{-2}$.

7. Decomposition of K_1, K_2, K_3 into spherical harmonics

Using standard techniques it is easy to show that:

$$\begin{aligned}
\alpha_x^2\alpha_y^2 + \alpha_x^2\alpha_z^2 + \alpha_y^2\alpha_z^2 &= \frac{2\sqrt{\pi}}{5}Y_0^0(\theta,\phi) - \frac{2\sqrt{\pi}}{15}\mathbf{Y}_4^C \\
\alpha_x^2\alpha_y^2\alpha_z^2 &= \frac{2\sqrt{\pi}}{105}Y_0^0(\theta,\phi) - \frac{2\sqrt{\pi}}{165}\mathbf{Y}_4^C + \frac{4}{231}\sqrt{\frac{\pi}{13}}\mathbf{Y}_6^C \\
\alpha_x^4\alpha_y^4 + \alpha_x^4\alpha_z^4 + \alpha_y^4\alpha_z^4 &= \frac{2\sqrt{\pi}}{35}Y_0^0(\theta,\phi) - \frac{16\sqrt{\pi}}{715}\mathbf{Y}_4^C - \frac{8}{385}\sqrt{\frac{\pi}{13}}\mathbf{Y}_6^C + \frac{2}{65}\sqrt{\frac{\pi}{17}}\mathbf{Y}_8^C.
\end{aligned} \tag{21}$$

Note that, in contrast to the multipolar approach developed above, all three expressions are characterized by tensors of mixed rank. In particular, the K_3 term contains tensors of rank 0, 4, 6, and 8. Thus care must be exercised in fitting any data with the K_1, K_2, and K_3 anisotropy terms, since they do not form a basis set. Note also that for finite K_3 the anisotropy will show a small eightfold symmetry in the [001]-plane.

Using equation (21), the anisotropy energy of equation (1) can be re-written in the concise form

$$\begin{aligned}
E_A = \frac{2\sqrt{\pi}}{5}&\left(K_1 + \frac{1}{21}K_2 + \frac{1}{7}K_3\right)Y_0^0(\theta,\phi) \\
&- \frac{2\sqrt{\pi}}{15}\left(K_1 + \frac{1}{11}K_2 + \frac{24}{143}K_3\right)\mathbf{Y}_4^C \\
&+ \frac{4}{231}\sqrt{\frac{\pi}{13}}\left(K_2 - \frac{6}{5}K_3\right)\mathbf{Y}_6^C \\
&+ \frac{2}{65}\sqrt{\frac{\pi}{17}}K_3\mathbf{Y}_8^C.
\end{aligned} \tag{22}$$

On comparing equations (19) and (22) therefore, and ignoring all terms which transform with $N > 8$, we find

$$\begin{aligned}
\tilde{K}_0 &= \frac{2\sqrt{\pi}}{5}\left(K_1 + \frac{1}{21}K_2 + \frac{1}{7}K_3\right)\\
\tilde{K}_4 &= -\frac{2\sqrt{\pi}}{15}\left(K_1 + \frac{1}{11}K_2 + \frac{24}{143}K_3\right)\\
\tilde{K}_6 &= +\frac{4}{231}\sqrt{\frac{\pi}{13}}\left(K_2 - \frac{6}{5}K_3\right)\\
\tilde{K}_8 &= +\frac{2}{65}\sqrt{\frac{\pi}{17}}K_3.
\end{aligned} \tag{23}$$

Finally, on ignoring the constant terms, and inverting equation (23), we obtain

$$\begin{aligned}
K_1 &= -\frac{15}{2\sqrt{\pi}}\tilde{K}_4 - \frac{21}{4}\sqrt{\frac{13}{\pi}}\tilde{K}_6 - \frac{9}{1}\sqrt{\frac{17}{\pi}}\tilde{K}_8\\
K_2 &= +\frac{231}{4}\sqrt{\frac{13}{\pi}}\tilde{K}_6 + \frac{39}{1}\sqrt{\frac{17}{\pi}}\tilde{K}_8\\
K_3 &= +\frac{65}{2}\sqrt{\frac{17}{\pi}}\tilde{K}_8.
\end{aligned} \tag{24}$$

This is essentially the approach adopted by A&D since they do not consider terms higher than K_3.

As stated earlier, all the multi-polar anisotropy constants $\tilde{K}_N$ decrease monotonically with increasing temperature, with $\tilde{K}_N$ decreasing more rapidly than $\tilde{K}_{N-1}$. Thus we can immediately conclude, from an examination of equation (24), that while changes of sign could occur in K_1 and K_2, this cannot happen with K_3, which decreases monotonically with temperature. These observations are born out by the calculations presented in the next section.

8. Calculated values of K_1, K_2, and K_3

Using equations (19) and (20) together with equation (24) the phenomenological constants K_1, K_2 and K_3 can be obtained. The temperature dependent anisotropy parameters can be seen in figures 6–10, again in logarithmic form. Four of these diagrams should be compared to figures 10–13 ($TbFe_2$–$ErFe_2$) of A&D. The agreement is astonishing and gives credence to the theory. Note that K_3 decreases monotonically with increasing temperature for all the REs in question. This can be understood by reference to equation (24), which shows that K_3 is directly proportional to $\tilde{K}_8$. We now discuss each $REFe_2$ in turn.

In the case of $TbFe_2$, the calculations shows that all the multipolar coefficients $\tilde{K}_N$ are positive (see figure 1). Thus from equation (24) we deduce that K_1 is negative, with both K_2 and K_3 positive. No cancellation of terms can occur. Consequently, $TbFe_2$ 'appears' to be in accord with expectations based on the C&C model.

In the case of $DyFe_2$, $\tilde{K}_8$, $\tilde{K}_{10}$, and $\tilde{K}_{12}$ are positive, with $\tilde{K}_4$ and $\tilde{K}_6$ negative. As a result, K_2 changes sign due to competition between $\tilde{K}_6$ and $\tilde{K}_8$. At low temperatures the $\tilde{K}_8$ term dominates, but because it falls more quickly than $\tilde{K}_6$ a change in the sign of K_2 takes place. Note that this behaviour could not occur in the absence of $K_3(\propto\tilde{K}_8)$. Note also that K_3 is larger than both K_1 and K_2 at low temperatures, in accord with the calculations of A&D.

For $HoFe_2$, $\tilde{K}_6$, $\tilde{K}_8$, and $\tilde{K}_{12}$ are all positive with $\tilde{K}_4$ and $\tilde{K}_{10}$ negative. In the case of K_2, both $\tilde{K}_6$ and $\tilde{K}_8$ possess the same sign (positive). So their combined effect is additive. However, in the case of K_1, both $-\tilde{K}_6$ and $-\tilde{K}_8$ are now negative (see equation (24)) and in competition with the now positive $-\tilde{K}_4$ term. At low temperatures $\tilde{K}_6$ and $\tilde{K}_8$ dominate, but

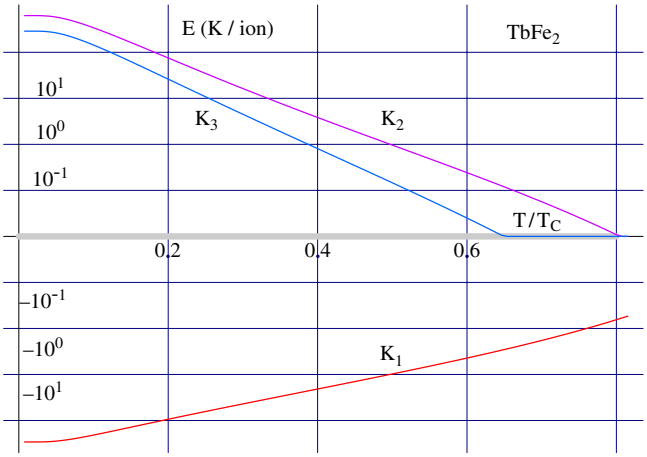

Figure 6. The calculated bulk magnetic anisotropy constants K_1, K_2, and K_3 for $TbFe_2$, plotted logarithmically, as a function of reduced temperature T/T_C. The thick line corresponds to the region $-10^{-2} \leqslant |K_i| \leqslant +10^{-2}$.

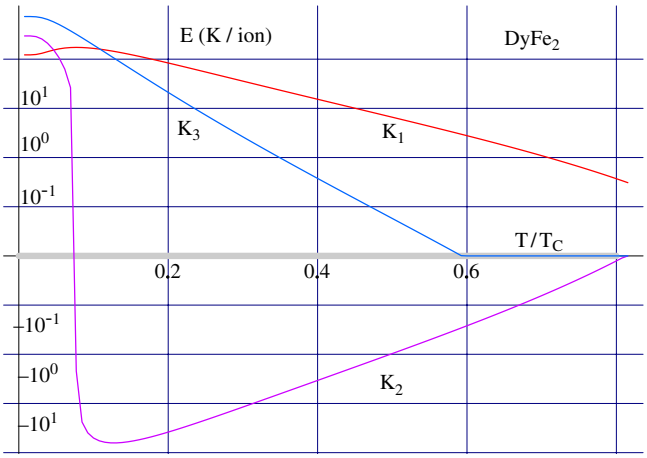

Figure 7. The calculated bulk magnetic anisotropy constants K_1, K_2, and K_3 for $DyFe_2$, plotted logarithmically, as a function of reduced temperature T/T_C. The thick line corresponds to the region $-10^{-2} \leqslant |K_i| \leqslant +10^{-2}$.

at higher temperatures the more slowly changing positive $-\tilde{K}_4$ term takes over, leading to a change in sign of K_1, from negative to positive, as the temperature is raised.

For $ErFe_2$ $\tilde{K}_4$, $\tilde{K}_8$, and $\tilde{K}_{12}$ are all positive, with $\tilde{K}_6$ and $\tilde{K}_{10}$ negative. $\tilde{K}_4$ is the dominant term, resulting in a negative K_1. In the case of K_2, the negative term $\tilde{K}_6$ is greater than the positive $\tilde{K}_8$ term, resulting in a negative K_2 coefficient. Note the crossover at about $T/T_C = \sim 0.2$. This 'crossover' was also witnessed by A&D, with K_2 dominant at low temperatures.

The results for $TmFe_2$ are very similar to those of $TbFe_2$, except that the temperature dependence of all the anisotropy constants is more rapid. This is due to the smaller magnetic exchange field at the Tm site. In $TbFe_2 X = 150$ K, whereas in $TmFe_2$ $X = 50$ K. The results for $TmFe_2$ are new.

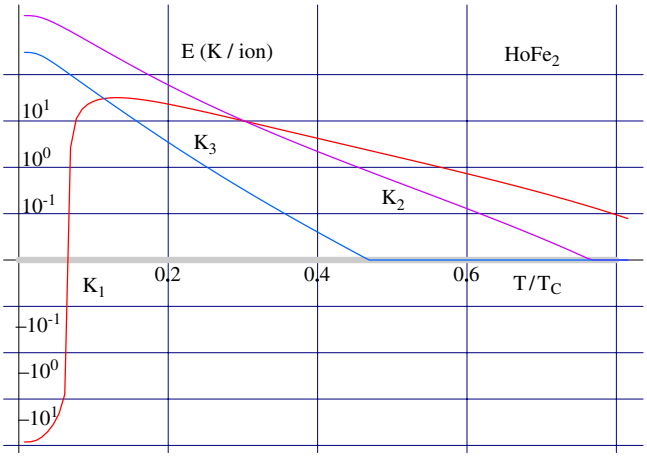

Figure 8. The calculated bulk magnetic anisotropy constants K_1, K_2, and K_3 for $HoFe_2$, plotted logarithmically, as a function of reduced temperature T/T_C. The thick line corresponds to the region $-10^{-2} \leqslant |K_i| \leqslant +10^{-2}$.

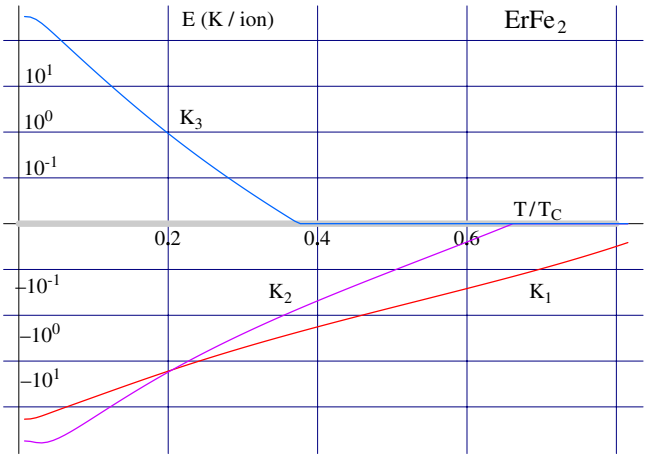

Figure 9. The calculated bulk magnetic anisotropy constants K_1, K_2, and K_3 for $ErFe_2$, plotted logarithmically, as a function of reduced temperature T/T_C. The thick line corresponds to the region $-10^{-2} \leqslant |K_i| \leqslant +10^{-2}$.

From the above, it is clear that the somewhat convoluted temperature dependence of the phenomenological coefficients K_1, K_2, K_3, etc is due primarily to the use of a non-orthogonal basis set. This leads to mixtures of the multipolar coefficients $\tilde{K}_4$, $\tilde{K}_6$, and $\tilde{K}_8$, with differing temperature dependences. However, all of these difficulties disappear if we elect to use the multipolar treatment of magnetic anisotropy, in place of the phenomenological approach. Finally, we remark that it is possible to implement the multipolar approach using direction cosines. The appropriate expressions are contained in appendix B.

This concludes our discussion of magnetic anisotropy within the phenomenological approach, constrained by K_1, K_2, and K_3. In the next section, the phenomenological approach is extended to include K_4 and K_5 anisotropy terms. As we shall see, this leads to significant changes in figures 6–10 for $TbFe_2$ to $TmFe_2$.

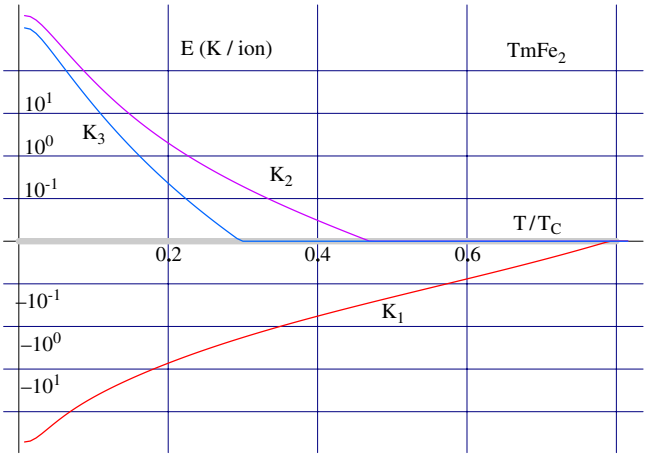

Figure 10. The calculated bulk magnetic anisotropy constants K_1, K_2, and K_3 for $TmFe_2$, plotted logarithmically, as a function of reduced temperature T/T_C. The thick line corresponds to the region $-10^{-2} \leqslant |K_i| \leqslant +10^{-2}$.

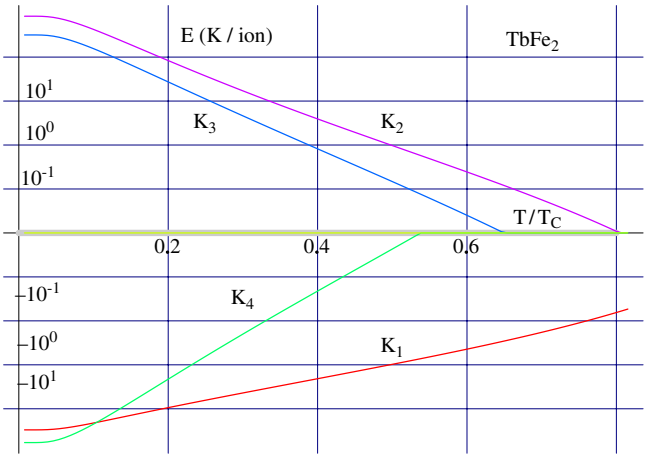

Figure 11. The calculated bulk magnetic anisotropy constants K_1, K_2, K_3, and K_4 for $TbFe_2$, plotted logarithmically, as a function of reduced temperature T/T_C. K_5 is negligible. The thick line corresponds to the region $-10^{-2} \leqslant |K_i| \leqslant +10^{-2}$.

9. Higher order phenomenological terms K_4 and K_5

Within the phenomenological framework, it is difficult to establish preferred forms for the higher order terms K_4 and K_5, because we are not dealing with a basis set. We choose to write

$$E_A = K_1\left[\alpha_x^2\alpha_y^2 + \alpha_x^2\alpha_z^2 + \alpha_y^2\alpha_z^2\right] + K_2\left[\alpha_x^2\alpha_y^2\alpha_z^2\right] + K_3\left[\alpha_x^4\alpha_y^4 + \alpha_x^4\alpha_z^4 + \alpha_y^4\alpha_z^4\right] + K_4\left[\alpha_x^4\alpha_y^4\alpha_z^2 + \alpha_x^4\alpha_y^2\alpha_z^4 + \alpha_x^2\alpha_y^4\alpha_z^4\right] + K_5\left[\alpha_x^4\alpha_y^4\alpha_z^4\right]. \quad (25)$$

In essence, the K_4 term is simply the product of the K_1 and K_2 terms, while the K_5 term is the K_2 term squared. Thus from a computational point of view these terms should be relatively easy to implement.

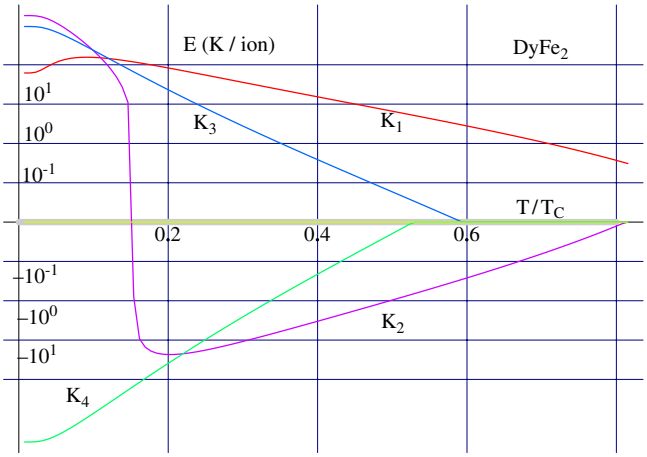

Figure 12. The calculated bulk magnetic anisotropy constants K_1, K_2, K_3, and K_4 for $DyFe_2$, plotted logarithmically, as a function of reduced temperature T/T_C. K_5 is negligible. The thick line corresponds to the region $-10^{-2} \leqslant |K_i| \leqslant +10^{-2}$.

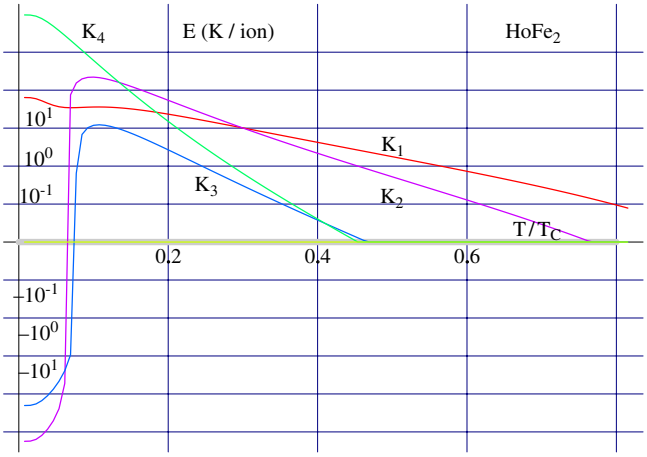

Figure 13. The calculated bulk magnetic anisotropy constants K_1, K_2, K_3, and K_4 for $HoFe_2$, plotted logarithmically, as a function of reduced temperature T/T_C. K_5 is negligible. The thick line corresponds to the region $-10^{-2} \leqslant |K_i| \leqslant +10^{-2}$.

Using standard decomposition techniques it is easy to show that

$$\left[\alpha_x^4\alpha_y^4\alpha_z^2 + \alpha_x^4\alpha_y^2\alpha_z^4 + \alpha_x^2\alpha_y^4\alpha_z^4\right] = \frac{2\sqrt{\pi}}{385}Y_0^0(\theta,\phi) - \frac{8\sqrt{\pi}}{2145}\mathbf{Y}_4^C(\theta,\phi) + \frac{36}{6545}\sqrt{\frac{\pi}{13}}\mathbf{Y}_6^C(\theta,\phi) + \frac{2}{1235}\sqrt{\frac{\pi}{17}}\mathbf{Y}_8^C(\theta,\phi) - \frac{4}{3553}\sqrt{\frac{\pi}{21}}\mathbf{Y}_{10}^C(\theta,\phi) \tag{26}$$

and

$$\left[\alpha_x^4\alpha_y^4\alpha_z^4\right] = \frac{2\sqrt{\pi}}{5005}Y_0^0(\theta,\phi) - \frac{4\sqrt{\pi}}{12\,155}\mathbf{Y}_4^C(\theta,\phi) + \frac{72}{124\,355}\sqrt{\frac{\pi}{13}}\mathbf{Y}_6^C(\theta,\phi) + \frac{2}{8645}\sqrt{\frac{\pi}{17}}\mathbf{Y}_8^C(\theta,\phi) - \frac{8}{81\,719}\sqrt{\frac{3\pi}{7}}\mathbf{Y}_{10}^C(\theta,\phi) + \frac{48\sqrt{\pi}}{3380\,195}\mathbf{Y}_{12}^C(\theta,\phi). \tag{27}$$

Thus equation (24) becomes

$$E_A = \frac{2\sqrt{\pi}}{5}\left(K_1 + \frac{1}{21}K_2 + \frac{1}{7}K_3 + \frac{1}{77}K_4 + \frac{1}{1001}K_5\right)Y_0^0(\theta,\phi)$$
$$- \frac{2\sqrt{\pi}}{15}\left(K_1 + \frac{1}{11}K_2 + \frac{24}{143}K_3 + \frac{4}{143}K_4 + \frac{6}{2431}K_5\right)\mathbf{Y}_4^C(\theta,\phi)$$
$$+ \frac{4}{231}\sqrt{\frac{\pi}{13}}\left(K_2 - \frac{6}{5}K_3 + \frac{27}{85}K_4 + \frac{54}{1615}K_5\right)\mathbf{Y}_6^C(\theta,\phi)$$
$$+ \frac{2}{65}\sqrt{\frac{\pi}{17}}\left(K_3 + \frac{1}{19}K_4 + \frac{1}{133}K_5\right)\mathbf{Y}_8^C(\theta,\phi)$$
$$- \frac{4}{3553}\sqrt{\frac{\pi}{21}}\left(K_4 + \frac{6}{23}K_5\right)\mathbf{Y}_{10}^C(\theta,\phi)$$
$$+ \frac{48\sqrt{\pi}}{3380\,195}K_5\mathbf{Y}_{12}^C(\theta,\phi) \tag{28}$$

with the inverse transformation

$$K_1 = -\frac{15}{2\sqrt{\pi}}\tilde{K}_4 - \frac{21}{4}\sqrt{\frac{13}{\pi}}\tilde{K}_6 - \frac{9}{1}\sqrt{\frac{17}{\pi}}\tilde{K}_8 - \frac{55}{4}\sqrt{\frac{21}{\pi}}\tilde{K}_{10} - \frac{195}{2\sqrt{\pi}}\tilde{K}_{12}$$
$$K_2 = +\frac{231}{4}\sqrt{\frac{13}{\pi}}\tilde{K}_6 + \frac{39}{1}\sqrt{\frac{17}{\pi}}\tilde{K}_8 + \frac{1353}{4}\sqrt{\frac{21}{\pi}}\tilde{K}_{10} + \frac{32\,045}{8\sqrt{\pi}}\tilde{K}_{12}$$
$$K_3 = \frac{65}{2}\sqrt{\frac{17}{\pi}}\tilde{K}_8 + \frac{187}{4}\sqrt{\frac{21}{\pi}}\tilde{K}_{10} + \frac{20\,995}{48\sqrt{\pi}}\tilde{K}_{12} \tag{29}$$
$$K_4 = -\frac{3553}{4}\sqrt{\frac{21}{\pi}}\tilde{K}_{10} - \frac{146\,965}{8\sqrt{\pi}}\tilde{K}_{12}$$
$$K_5 = +\frac{3380\,195}{48\sqrt{\pi}}\tilde{K}_{12}.$$

The revised set of graphs based on equation (29) can be seen in figures 11–15. These should be compared with figures 6–10, respectively. There are significant differences. One, the new anisotropy constant K_4 cannot be ignored. Two, at low temperatures K_4 is larger than K_3 in all cases. Three, K_4 decreases monotonically, with increasing temperature. Four, K_5 is negligible ($|K_5| < 10^{-2}$). There are also significant changes in the other coefficients K_1, K_2, and K_3. This is most marked in $HoFe_2$, where it will be seen that both K_1 and K_3 now change sign. Finally, we remark that the parameters given in figures 1–5 and figures 11–15 represent an advance on earlier work.

10. Conclusions

In this paper, it has been shown that despite their high ordering temperatures of ∼650 K the original C&C model is insufficient for the $REFe_2$ compounds. However by extending the C&C model to second order in $\mathcal{H}_{CF}$, it is not only possible to replicate the results of A&D, but also to provide explanations for (i) the unexpected changes in sign of K_1 and K_2 in $HoFe_2$ and $DyFe_2$, respectively, and (ii) the origin and behaviour of the K_3 term, witnessed by these

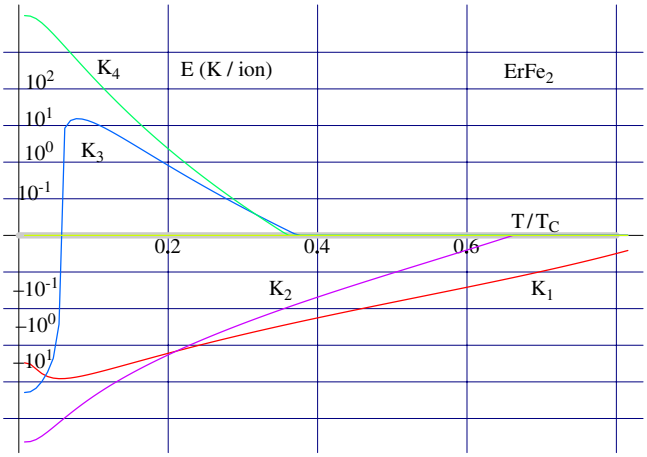

Figure 14. The calculated bulk magnetic anisotropy constants K_1, K_2, K_3, and K_4 for $ErFe_2$, plotted logarithmically, as a function of reduced temperature T/T_C. K_5 is negligible. The thick line corresponds to the region $-10^{-2} \leqslant |K_i| \leqslant +10^{-2}$.

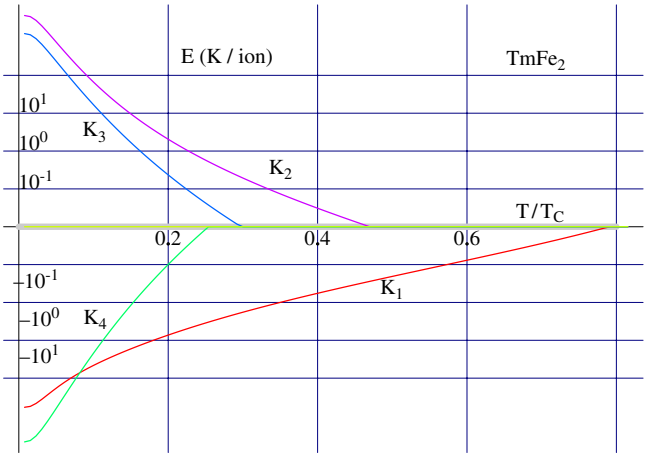

Figure 15. The calculated bulk magnetic anisotropy constants K_1, K_2, K_3, and K_4 for $TmFe_2$, plotted logarithmically, as a function of reduced temperature T/T_C. K_5 is negligible. The thick line corresponds to the region $-10^{-2} \leqslant |K_i| \leqslant +10^{-2}$.

authors. However, it has also been shown that the higher order term K_4 is important, exceeding that of K_3 at low temperatures. Moreover, the inclusion of K_4 leads to significant changes in the values of K_1, K_2, and K_3.

Finally, we stress that, from a theoretical point of view at least, the multipolar approach to magnetic anisotropy in the $REFe_2$ compounds confers significant advantages over the phenomenological method. All the $\tilde{K}_N$ ($N = 4, 6, 8, 10, 12$) multi-polar anisotropy coefficients decrease monotonically with increasing temperature, with $\tilde{K}_N$ reaching 'zero' before $\tilde{K}_{N-2}$ etc. These results are in accord with expectations based on the original C&C model.

Appendix A. Calculation of the $\alpha_{n,n',N}(T)$ coefficients

From equation (16) we have

$$\alpha_{n,n',N}(T) = \sum_q \begin{pmatrix} n & n' & N \\ q & -q & 0 \end{pmatrix} \left\langle \mathbf{T}^n_q : \mathbf{T}^{n'}_{-q} \right\rangle. \tag{A.1}$$

Also, from equations (42)–(44) of Bowden (1977),

$$\langle \mathbf{T}^n_0 : \mathbf{T}^{n'}_0 \rangle = \langle \mathbf{T}^n_0 \mathbf{T}^{n'}_0 \rangle - \langle \mathbf{T}^n_0 \rangle \langle \mathbf{T}^{n'}_0 \rangle \tag{A.2}$$

and

$$\langle \mathbf{T}^n_q : \mathbf{T}^{n'}_{-q} \rangle = \left(\frac{\exp[\beta X q] - 1}{\beta X q} \right) \langle \mathbf{T}^n_q \mathbf{T}^{n'}_{-q} \rangle = \left(\frac{1 - \exp[-\beta X q]}{\beta X q} \right) \langle \mathbf{T}^{n'}_{-q} \mathbf{T}^n_q \rangle \qquad q \neq 0 \tag{A.3}$$

where we have made use of the identity

$$\langle \mathbf{T}^n_q \mathbf{T}^{n'}_{-q} \rangle = \exp[-\beta X q] \langle \mathbf{T}^{n'}_{-q} \mathbf{T}^n_q \rangle. \tag{A.4}$$

So the $\alpha_{n,n',N}(T)$ coefficients can be rewritten:

$$\begin{aligned} \alpha_{n,n',N}(T) = {} & \begin{pmatrix} n & n' & N \\ 0 & 0 & 0 \end{pmatrix} \{ \langle \mathbf{T}^n_0 \mathbf{T}^{n'}_0 \rangle - \langle \mathbf{T}^n_0 \rangle \langle \mathbf{T}^{n'}_0 \rangle \} \\ & + \sum_{q>0} \begin{pmatrix} n & n' & N \\ q & -q & 0 \end{pmatrix} \left(\frac{1 - \exp[-\beta X q]}{\beta X q} \right) \\ & \times \{ \langle \mathbf{T}^{n'}_{-q} \mathbf{T}^n_q \rangle + (-1)^{n+n'+N} \langle \mathbf{T}^n_{-q} \mathbf{T}^{n'}_q \rangle \}. \end{aligned} \tag{A.5}$$

At very low temperatures, the diagonal term in equation (A.5) vanishes. Thus we can write

$$\alpha_{n,n',N}(T \to 0\ \mathrm{K}) = \frac{1}{\beta X} \gamma_{n,n',N} \tag{A.6}$$

where (i)

$$\gamma_{n,n',N} = \sum_{q>0} \frac{1}{q} \begin{pmatrix} n & n' & N \\ q & -q & 0 \end{pmatrix} \{ \langle -J | \mathbf{T}^{n'}_{-q} \mathbf{T}^n_q + \mathbf{T}^n_{-q} \mathbf{T}^{n'}_q | -J \rangle \} \tag{A.7}$$

(ii) $|J_z = -J\rangle$ is the ground state, and (iii) N is even. Values of the $\gamma_{n,n',N}$ can be seen in table A.1. Note that the temperature dependent term $1/\beta$ in equation (A.6) will cancel the β term appearing outside the outer brackets in equation (15).

Finally, we observe that the coefficients in table A.1, together with equation (A.6), and table 1 of the main text can be used to establish the intercepts of the second order multipolar constants $\tilde{K}''_{nn'N}(T = 0\ \mathrm{K})$. For Dy we obtain for all the second order contributions

$$\begin{aligned} \tilde{K}''_4(0\ \mathrm{K}) &= \frac{1}{2X} \left[-\frac{1044\,000\sqrt{\pi}}{11} \tilde{B}^2_4 - \frac{12\,801\,600}{1} \sqrt{\frac{30\pi}{11}} \tilde{B}_4 \tilde{B}_6 + \frac{3019\,086\,000\sqrt{\pi}}{17} \tilde{B}^2_6 \right] \\ \tilde{K}''_6(0\ \mathrm{K}) &= \frac{1}{2X} \left[\frac{1782\,720\sqrt{13\pi}}{77} \tilde{B}^2_4 - \frac{6822\,900}{17} \sqrt{\frac{390\pi}{11}} \tilde{B}_4 \tilde{B}_6 - \frac{886\,032\,000\sqrt{13\pi}}{323} \tilde{B}^2_6 \right] \\ \tilde{K}''_8(0\ \mathrm{K}) &= \frac{1}{2X} \left[\frac{1336\,770}{1} \sqrt{\frac{\pi}{17}} \tilde{B}^2_4 + \frac{38\,593\,800\sqrt{17\pi}}{19} \tilde{B}_4 \tilde{B}_6 + \frac{1714\,395\,375\sqrt{17\pi}}{19} \tilde{B}^2_6 \right] \\ \tilde{K}''_{10}(0\ \mathrm{K}) &= \frac{1}{2X} \left[\frac{117\,602\,550\sqrt{770\pi}}{323} \tilde{B}_4 \tilde{B}_6 - \frac{274\,155\,131\,250\sqrt{21\pi}}{7429} \tilde{B}^2_6 \right] \\ \tilde{K}''_{12}(0\ \mathrm{K}) &= \frac{1}{X} \left[\frac{1489\,138\,752\,025\sqrt{\pi}}{7429} \tilde{B}^2_6 \right]. \end{aligned} \tag{A.8}$$

Table A.1. The coefficients $\gamma_{n,n',N}$ for $J = 15/2$.

$j = 15/2$	γ_{440}	γ_{444}	γ_{446}	γ_{448}		
	$\frac{1199\,250}{1}$	$\frac{130\,500}{1}\sqrt{\frac{26}{77}}$	$\frac{44\,568}{1}\sqrt{\frac{65}{11}}$	$-\frac{311\,913}{1}\sqrt{\frac{130}{187}}$		
	γ_{460}	γ_{464}	γ_{466}	γ_{468}	γ_{4610}	
	0	$\frac{-400\,050\sqrt{78}}{1}$	$-\frac{81\,225}{1}\sqrt{\frac{2730}{17}}$	$\frac{1\,378\,350}{1}\sqrt{\frac{1365}{323}}$	$-\frac{1507\,725}{1}\sqrt{\frac{3003}{323}}$	
	γ_{660}	γ_{664}	γ_{666}	γ_{668}	γ_{6610}	γ_{6612}
	$\frac{230\,509\,125\sqrt{13}}{1}$	$\frac{5134\,500}{1}\sqrt{\frac{1001}{17}}$	$\frac{55\,377\,000}{1}\sqrt{\frac{143}{323}}$	$-\frac{2473\,875}{1}\sqrt{\frac{17\,017}{38}}$	$\frac{301\,269\,375}{1}\sqrt{\frac{273}{7429}}$	$-\frac{705\,827\,925}{1}\sqrt{\frac{91}{7429}}$

On substituting for $\tilde{B}_4$, $\tilde{B}_6$, and X from table 1 we find

$$\begin{aligned}
&\tilde{K}_4''(0\text{ K}) = -6.001\text{ (K/ion)}\\
&\tilde{K}_6''(0\text{ K}) = 1.403\\
&\tilde{K}_8''(0\text{ K}) = 9.732\\
&\tilde{K}_{10}''(0\text{ K}) = 1.697\\
&\tilde{K}_{12}''(0\text{ K}) = 0.225.
\end{aligned} \tag{A.9}$$

Note that the intercepts $\tilde{K}_8''(0\text{ K})$, $\tilde{K}_{10}''(0\text{ K})$, and $\tilde{K}_{12}''(0\text{ K})$ are all positive and in agreement with figure 7. For the other two intercepts we must add in the first order terms:

$$\begin{aligned}
&\tilde{K}_4'(0\text{ K}) = 117\sqrt{70}\tilde{B}_4 = -49.468\text{ (K/ion)}\\
&\tilde{K}_6'(0\text{ K}) = 975\sqrt{231}\tilde{B}_6 = -6.505.
\end{aligned} \tag{A.10}$$

Note that (i) the second order term $\tilde{K}_8''(0\text{ K})$ is larger than first order term $\tilde{K}_6'(0\text{ K})$, (ii) the second order term $\tilde{K}_4''(0\text{ K})$ augments the first order term $\tilde{K}_4'(0\text{ K})$ by some 12%, and (iii) $\tilde{K}_6''(0\text{ K})$ reduces the first order term $\tilde{K}_6'(0\text{ K})$ by some 21.5%. Similar but differing remarks can be made concerning the other four rare earths.

Appendix B. Cubic combinations of spherical harmonics in terms of direction cosines

The cubic multipolar combination of spherical harmonics can be re-expressed in terms of direction cosines:

$$\begin{aligned}
\mathbf{Y}_4^C &= \frac{3}{2\sqrt{\pi}}\{1 - 5[\alpha_x^2\alpha_y^2 + \alpha_x^2\alpha_z^2 + \alpha_y^2\alpha_z^2]\} = \frac{3}{4\sqrt{\pi}}\{5[\alpha_x^4 + \alpha_y^4 + \alpha_z^4] - 3\}\\
\mathbf{Y}_6^C &= \frac{1}{4}\sqrt{\frac{13}{\pi}}\{2 - 21(\alpha_x^2\alpha_y^2 + \alpha_x^2\alpha_z^2 + \alpha_y^2\alpha_z^2) + 231\alpha_x^2\alpha_y^2\alpha_z^2\}\\
\mathbf{Y}_8^C &= \frac{1}{2}\sqrt{\frac{17}{\pi}}\{1 - 18(\alpha_x^2\alpha_y^2 + \alpha_x^2\alpha_z^2 + \alpha_y^2\alpha_z^2) + 65(\alpha_x^4\alpha_y^4 + \alpha_x^4\alpha_z^4 + \alpha_y^4\alpha_z^4) + 78\alpha_x^2\alpha_y^2\alpha_z^2\}\\
\mathbf{Y}_{10}^C &= -\frac{1}{4}\sqrt{\frac{21}{\pi}}\{-2 + 55(\alpha_x^2\alpha_y^2 + \alpha_x^2\alpha_z^2 + \alpha_y^2\alpha_z^2) - 187(\alpha_x^4\alpha_y^4 + \alpha_x^4\alpha_z^4 + \alpha_y^4\alpha_z^4)\\
&\qquad - 1353\alpha_x^2\alpha_y^2\alpha_z^2 + 3553(\alpha_x^2\alpha_y^4\alpha_z^4 + \alpha_x^4\alpha_y^2\alpha_z^4 + \alpha_x^4\alpha_y^4\alpha_z^2)\}\\
\mathbf{Y}_{12}^C &= -\frac{1}{48\sqrt{\pi}}\{5[24 - 936(\alpha_x^2\alpha_y^2 + \alpha_x^2\alpha_z^2 + \alpha_y^2\alpha_z^2)\\
&\qquad + 4199(\alpha_x^4\alpha_y^4 + \alpha_x^4\alpha_z^4 + \alpha_y^4\alpha_z^4) + 38454\alpha_x^2\alpha_y^2\alpha_z^2\\
&\qquad - 176\,358(\alpha_x^2\alpha_y^4\alpha_z^4 + \alpha_x^4\alpha_y^2\alpha_z^4 + \alpha_x^4\alpha_y^4\alpha_z^2) + 676039\alpha_x^4\alpha_y^4\alpha_z^4].\}
\end{aligned} \tag{B.1}$$

The right-hand sides of these equations can be rewritten in various forms using the identities

$$\begin{aligned}
&\alpha_x^2\alpha_y^2 + \alpha_x^2\alpha_z^2 + \alpha_y^2\alpha_z^2 = \tfrac{1}{2}[1 - (\alpha_x^4 + \alpha_y^4 + \alpha_z^4)] \\
&\alpha_x^2\alpha_y^2\alpha_z^2 = \tfrac{1}{6}[1 - 3(\alpha_x^4 + \alpha_y^4 + \alpha_z^4) + 2(\alpha_x^6 + \alpha_y^6 + \alpha_z^6)] \qquad \text{(B.2)} \\
&\alpha_x^4\alpha_y^4 + \alpha_x^4\alpha_z^4 + \alpha_y^4\alpha_z^4 = \tfrac{1}{6}[2 + 6(\alpha_x^4 + \alpha_y^4 + \alpha_z^4) - 8(\alpha_x^6 + \alpha_y^6 + \alpha_z^6) + 3(\alpha_x^8 + \alpha_y^8 + \alpha_z^8)1].
\end{aligned}$$

References

Abragam A and Bleaney B 1970 *Electron Paramagnetic Resonance of Transition Ions* (Oxford: Clarendon)

Akulov N Z 1936 *Z. Phys.* **100** 197

Amato M, Retorri A and Pini M G 2000 *Physica* B **275** 120–3

Atzmony U and Dariel M P 1976 *Phys. Rev.* B **13** 4006–14

Atzmony U, Dariel M P, Bauminger E R, Lebenbaum D, Nowik I and Ofer S 1973 *Phys. Rev.* B **7** 4220–32

Aubert G 1968 *J. Appl. Phys.* **39** 504

Bleaney B, Bowden G J, Cadogan J M, Day R K and Dunlop J B 1981 *J. Phys. F: Met. Phys.* **12** 795–811

Bowden G J 1977 *J. Phys. F: Met. Phys.* **7** 1731–46

Bowden G J, Beaujour J-M L, Gordeev S, de Groot P A J, Rainford B D and Sawicki M 2000 *J. Phys.: Condens. Matter* **12** 9335–46

Bowden G J, Beaujour J-M L, Zhukov A A, Rainford B D, de Groot P A J, Ward R C C and Wells M R 2003 *J. Appl. Phys.* **93** 6480–2

Bowden G J, Bunbury D St P, Guimares A P and Synder R E 1968 *J. Phys. C: Solid State Phys.* **1** 1376–87

Bowden G J, de Groot P A J, O'Neil J D, Rainford B D and Zhukov A A 2004 *J. Phys.: Condens. Matter* **16** 2437–46

Bowden G J and Hutchison W D 1986 *J. Magn. Reson.* **67** 403–15

Buckmaster H A, Chatterjee R and Shing Y H 1972 *Phys. Status Solidi* **13** 9

Callen H B and Callen E 1965 *Phys. Rev.* **139** A455–71

Callen H B and Callen E 1966 *J. Phys. Chem. Solids* **27** 1271–85

Callen H B and Shtrikman S 1965 *Solid State Commun.* **3** 5–8

Clark A E 1979 *Handbook on the Physics and Chemistry of Rare Earths* vol 2, ed K A Gchneider and L Eyring (Amsterdam: North-Holland) chapter 15

Coey J M D and Skomski R 1993 *Phys. Scr.* T **49** 315

Cohen R L 1964 *Phys. Rev.* **134** A94–8

Dumesnil K, Dufour C, Mangin Ph, Rogalev A and Wilhelm F 2005 *J. Phys.: Condens. Matter* **17** L215–22

Dumesnil K, Dutheil M, Dufour C and Mangin Ph 2000 *Phys. Rev.* B **62** 1136–40

Edmonds A R 1957 *Angular Momentum in Quantum Mechanics* (Princeton, NJ: Princeton University Press)

Fullerton E E, Jiang J S and Bader S D 1999 *J. Magn. Magn. Mater.* **200** 392–404

Gordeev S, Beaujour J-M L, Bowden G J, de Groot P A J, Rainford B D, Ward R C C and Wells M R 2001 *J. Appl. Phys.* **89** 6828–30

Gordeev S N, Beaujour J-M L, Bowden G J, Rainford B D, de Groot P A J, Ward R C C, Wells M R and Jensen A G 2001 *Phys. Rev. Lett.* **87** 186808

Hutchings M T 1964 *Solid State Phys.* **16** 227

Mougin A, Dufour C, Dumesnil K and Mangin Ph 2000 *Phys. Rev.* B **62** 9517–31

Sawicki M, Bowden G J, de Groot P A J, Rainford B R, Beaujour J-M L, Ward R C C and Wells M R 2000 *Phys. Rev.* B **62** 5817–20

Smith D and Thornley J H M 1966 *Proc. R. Soc.* **89** 779–81